Hindawi Publishing Corporation
EURASIP Journal on Applied Signal Processing
Volume 2006, Article ID 39657, Pages 1–9
DOI 10.1155/ASP/2006/39657

From Matched Spatial Filtering towards the Fused Statistical Descriptive Regularization Method for Enhanced Radar Imaging

Yuriy Shkvarko

Cinvestav Unidad Guadalajara, Apartado Postal 31-438, Guadalajara, Jalisco 45090, Mexico

Received 20 June 2005; Revised 4 November 2005; Accepted 23 November 2005

Recommended for Publication by Douglas Williams

We address a new approach to solve the ill-posed nonlinear inverse problem of high-resolution numerical reconstruction of the spatial spectrum pattern (SSP) of the backscattered wavefield sources distributed over the remotely sensed scene. An array or synthesized array radar (SAR) that employs digital data signal processing is considered. By exploiting the idea of combining the statistical minimum risk estimation paradigm with numerical descriptive regularization techniques, we address a new fused statistical descriptive regularization (SDR) strategy for enhanced radar imaging. Pursuing such an approach, we establish a family of the SDR-related SSP estimators, that encompass a manifold of existing beamforming techniques ranging from traditional matched filter to robust and adaptive spatial filtering, and minimum variance methods.

1. INTRODUCTION

In this paper, we address a new approach to enhanced array radar or SAR imaging stated and treated as an ill-posed nonlinear inverse problem. The problem at hand is to perform high-resolution reconstruction of the power spatial spectrum pattern (SSP) of the wavefield sources scattered from the probing surface (referred to as a desired image). The reconstruction is to be performed via space-time processing of finite dimensional recordings of the remotely sensed data signals distorted in a stochastic measurement channel.

The SSP is defined as a spatial distribution of the power (i.e., the second-order statistics) of the random wavefield backscattered from the remotely sensed scene observed through the integral transform operator [1, 2]. Such operator is explicitly specified by the employed radar signal modulation and is traditionally referred to as the signal formation operator (SFO) [2, 3]. Moreover, in all practical remote sensing scenarios, the backscattered signals are contaminated with noise, that is, randomly distorted. Next, all digital signal recording schemes employ data sampling and quantization operations [2, 4], that is, projection of the continuous-form observations onto the finite dimensional data approximation subspaces; thus an inevitable loss of information is induced when performing such practical array data recordings. That is why the problem at hand has to be qualified and treated as a statistical ill-conditioned nonlinear inverse problem. Because of the stochastic nature and nonlinearity, *no unique analytical method* exists for reconstructing the SSP from the finite dimensional measurement data in an analytic closed form, that is, via designing some nonlinear solution operator that produces the unique continuous estimate of the desired SSP [4]. Hence, the particular solution strategy to be developed and applied must unify the practical data observation method with some form of statistical or descriptive regularization that incorporates the a priori model knowledge about the SSP to alleviate the problem ill-posedness.

The classical imaging with array radar or SAR implies application of the method called "matched spatial filtering" to process the recorded data signals [4–6]. Stated formally [4], such a method implies application of the adjoint SFO to the recorded data, computation of the squared norm of a filter's outputs and their averaging over the actually recorded samples (the so-called *snapshots* [7]) of the independent data observations. Although a number of authors have proposed different linear and nonlinear postprocessing approaches to enhance the images formed using such matched estimator (see, e.g., [8–10, 16]), all those are not a direct inference from the Bayesian optimal estimation theory [1]. Other approaches had focused primarily on designing the constrained regularization techniques for improving the resolution of the closely

spaced components in the SSP obtained by ways different from matched spatial filtering [7, 10–12] but again without aggregating the regularization principles with the minimum risk estimation strategy.

In this study, we propose a new fused statistical descriptive regularization (SDR) approach for estimating the SSP that aggregates the statistical minimum risk inference paradigm [2, 3] with the descriptive regularization techniques [4, 13]. Pursuing such an approach, we establish a family of the robust SDR-related estimators that encompass a manifold of existing imaging techniques ranging from traditional array matched spatial filtering to high-resolution minimum variance adaptive array beamforming. We also present robust SDR-related imaging algorithms that manifest enhanced resolution of the numerically reconstructed array images with substantially decreased computational load. The efficiency of two particular SDR algorithms (the robust spatial filtering (RSF) algorithm and the adaptive spatial filtering (ASF) algorithm) is illustrated through computer simulations of reconstructing the digital images provided with the SAR operating in some typical remote sensing scenarios.

2. SSP ESTIMATION AS AN INVERSE PROBLEM

2.1. Problem statement

The generalized mathematical formulation of the problem at hand presented here is similar in notation and structure to that in [4, 14], and some crucial elements are repeated for convenience to the reader. Consider a remote sensing experiment performed with a coherent array imaging radar or SAR (radar/SAR) that is traditionally referred to as radar imaging (RI) problem [2, 4, 15]. Here, we employ the conventional narrowband space-time model of the radar/SAR signals [1, 2]. In such a model [2], the wavefield backscattered from the remotely sensed scene is associated with the time invariant complex random scattering function $e(\mathbf{x})$ distributed over the probing surface $X \ni \mathbf{x}$. The measurement data wavefield $u(\mathbf{y}) = s(\mathbf{y}) + n(\mathbf{y})$ consists of the echo signals s and additive noise n, and is available for observations and recordings within the prescribed time(t)-space($\mathbf{p}$) observation domain $Y = T \times P$; $t \in T$, $\mathbf{p} \in P$, where $\mathbf{y} = (t, \mathbf{p})^T$ defines the time-space points in Y. The model of the observation wavefield u is defined by specifying the stochastic equation of observation (EO) of an operator form [4]:

$$u = Se + n; \quad e \in E;\ u, n \in U;\ S : E \longrightarrow U. \tag{1}$$

Here, S is referred to as the regular signal formation operator (SFO). It defines the transform of random scattered signals $e(\mathbf{x}) \in E(X)$ distributed over the remotely sensed scene (probing surface) $X \ni \mathbf{x}$ into the echo signals $(Se(\mathbf{x}))(\mathbf{y}) \in U(Y)$ over the time-space observation domain $Y = T \times P$; $t \in T$, $\mathbf{p} \in P$. In the functional terms [4, 6], such transform is referred to as the operator $S : E \to U$ that maps the scene signal space E (the space of the signals scattered from the remotely sensed scene) onto the observation data signal space U. The energy of any signal in (1) is inevitably bounded; hence following the generalized mathematical formulation [3, 4], both spaces E and U must be considered as Hilbert signal spaces. The inner products in such Hilbert spaces are defined via the integrals [4, 14]

$$\begin{aligned} [e_1, e_2]_E &= \int_X e_1(\mathbf{x}) e_2^*(\mathbf{x}) d\mathbf{x}, \\ [u_1, u_2]_U &= \int_Y u_1(\mathbf{y}) u_2^*(\mathbf{y}) d\mathbf{y}, \end{aligned} \tag{2}$$

respectively, where asterisk stands for complex conjugate. Next, using these definitions (2), the metrics structures in both spaces are imposed as [4, 14]

$$\begin{aligned} d_E^2(e_1, e_2) &= \|e_1 - e_2\|_E^2 = [(e_1 - e_2), (e_1 - e_2)]_E \\ &= \int_X |e_1(\mathbf{x}) - e_2(\mathbf{x})|^2 d\mathbf{x}, \\ d_U^2(u_1, u_2) &= \|u_1 - u_2\|_U^2 = [(u_1 - u_2), (u_1 - u_2)]_U \\ &= \int_Y |u_1(\mathbf{y}) - u_2(\mathbf{y})|^2 d\mathbf{y}, \end{aligned} \tag{3}$$

respectively. The metrics structures (3) define the square distances $d_E^2(e_1, e_2)$ between arbitrary different elements $e_1, e_2 \in E$ and $d_U^2(u_1, u_2)$ between arbitrary $u_1, u_2 \in U$. These square distances are imposed by the corresponding squared norms $\|\cdot\|_E^2$ and $\|\cdot\|_U^2$ and are represented by the inner products at the right-hand side in (3). Equations (1)–(3) explicitly define the general functional formulation of the EO and specify the corresponding metrics structures in the scene signal space E and observation data space U, respectively. Applying these formulations, in the following text we will adhere ourselves to the concise inner product notations $[\cdot, \cdot]_E$ and $[\cdot, \cdot]_U$ implying their integral-form definitions given by (2).

The operator model (1) of the stochastic EO may be also rewritten in the conventional integral form [2, 4, 7] as

$$u(\mathbf{y}) = (Se(\mathbf{x}))(\mathbf{y}) + n(\mathbf{y}) = \int_X S(\mathbf{y}, \mathbf{x}) e(\mathbf{x}) d\mathbf{x} + n(\mathbf{y}). \tag{4}$$

The functional kernel $S(\mathbf{y}, \mathbf{x})$ of the SFO given by (4) defines the signal wavefield formation model. It is specified by the time-space modulation of signals employed in a particular imaging radar system [2, 7, 15].

All the fields e, n, u in (1), (4) are assumed to be zero-mean complex-valued Gaussian random fields. Next, we assume an incoherent nature of the backscattered field $e(\mathbf{x})$. This is naturally inherent to all RI experiments [2, 4, 7, 14, 15] and leads to the δ-form of the scattering field correlation function, $R_e(\mathbf{x}_1, \mathbf{x}_2) = B(\mathbf{x}_1)\delta(\mathbf{x}_1 - \mathbf{x}_2)$, where the averaged square, $B(\mathbf{x}) = \langle |e(\mathbf{x})|^2 \rangle$ (i.e., the second-order statistics of the complex scattering function $e(\mathbf{x})$), is referred to as the power scattering function or *spatial spectrum pattern* (SSP) of the remotely sensed scene $X \ni \mathbf{x}$.

The nonlinear SSP estimation problem implies reconstruction of the SSP $B(\mathbf{x})$ distributed over the probing surface $X \ni \mathbf{x}$ from the available finite dimensional array (synthesized array) measurements of the data wavefield $u(\mathbf{y}) \in U(Y)$ performed in some statistically optimal way. Recall that in this paper we intend to develop and follow the fused SDR strategy.

2.2. Projection statistical model of the data measurements

The formulation of the data discretization and sampling in this paper follows the unified formalism given in [3, 4, 14] that enables us to generalize the finite-dimensional approximations of (1), (4) independent of the particular system configuration and the method of data measurements and recordings employed.

Following [4], consider an array composed of L antenna elements characterized by a set of complex amplitude-phase tapering functions $\{\tau_l^*(\mathbf{p});\ l = 1,\dots,L\}$ (the complex conjugate is taken for convenience). In general, the tapering functions may be considered to be either identical or different for the different elements of the array. In practice, the antenna elements in an array (synthesized array) are always distanced in space (do not overlap); that is, the tapering functions $\{\tau_l(\mathbf{p})\}$ have the distanced supports in $P \ni \mathbf{p}$. Hence, $\{\tau_l(\mathbf{p})\}$ compose an orthogonal set because these tapering functions satisfy the orthogonal criteria: $[\tau_l, \tau_n]_U = \|\tau_l\|^2\delta_{ln}$ $\forall l, n = 1,\dots,L$, where δ_{ln} represents the Kronecker operator. Consider, next, that the sensor output signal in every spatial measurement channel is then converted to I samples at the outputs of the temporal filters defined by their impulse response functions $\{\chi_i^*(t);\ i = 1,\dots,I\}$. Without loss of generality [3, 4], the set $\{\chi_i(t)\}$ is also assumed to be orthogonal (e.g., via proper filter design and calibration [2, 7]); that is, $[\chi_i, \chi_j]_U = \|\chi_i\|^2\delta_{ij}$ for all $i, j = 1,\dots,I$.

The composition $\{h_m(\mathbf{y}) = \tau_l(\mathbf{p})\chi_i(t);\ m = (l,i) = 1,\dots,\ M = L \times I\}$ of all these $L \times I = M$ functions ordered by multiindex $m = (l,i)$ composes a set of orthogonal spatial-temporal weighting functions that explicitly determine the outcomes $\{U_m = [u, h_m]_U = \int_Y u(\mathbf{y})h_m^*(\mathbf{y})d\mathbf{y}; m = 1,\dots,M\}$ of such an M-dimensional (M-d in our notation) data recording channel.

Viewing it as an approximation problem leads one to the projection concept for a transformation of the continuous data field $u(\mathbf{y})$ to the $M\times 1$ vector $\mathbf{U} = (U_1,\dots,U_M)^T$ of sampled spatial-temporal data recordings. The M-d observations in the terms of projections [14] can be expressed as

$$u_{(M)}(\mathbf{y}) = (P_{U(M)}u)(\mathbf{y}) = \sum_{m=1}^{M} U_m\phi_m(\mathbf{y}) \tag{5}$$

with coefficients $\{U_m = [u, h_m]_U\}$, where $P_{U(M)}$ represents a projector onto the M-d observation subspace

$$U_{(M)} = P_{U(M)}U = \text{Span}\,\{\phi_m(\mathbf{y})\} \tag{6}$$

uniquely defined by a set of the orthogonal functions $\{\phi_m(\mathbf{y}) = \|h_m(\mathbf{y})\|^{-2}h_m(\mathbf{y});\ m = 1,\dots,M\}$ that are related to $\{h_m(\mathbf{y})\}$ as a dual basis in $U_{(M)}$; that is, $[h_m, \phi_n]_U = \delta_{mn}$ $\forall m, n = 1,\dots,M$.

In the observation scene $X \ni \mathbf{x}$, the discretization of the scattering field $e(\mathbf{x})$ is traditionally performed over a $Q \times N$ rectangular grid where Q defines the dimension of the grid over the horizontal (azimuth) coordinate x_1, and N defines the grid dimension over the orthogonal coordinate x_2 (the number of the range gates projected onto the scene). The discretized complex scattering function is represented by coefficients [14] $E_k = E_{(q,n)} = [e, g_k]_E = \int_x e(\mathbf{x})g_k(\mathbf{x})d\mathbf{x}$, $k = 1,\dots,K = Q\times N$, of its decomposition over the grid composed of such identical shifted rectangular functions $\{g_k(\mathbf{x}) = g_{(q,n)}(\mathbf{x}) = 1$ if $\mathbf{x} \in \rho_{(q,n)}(\mathbf{x}) = \text{rect}_{(q,n)}(x_1, x_2)$ and $g_k(\mathbf{x}) = 0$ for other $\mathbf{x} \notin \rho_{(q,n)}(\mathbf{x})$ for all $q = 1,\dots,Q,\ n = 1,\dots,N;\ k = 1,\dots,K = Q \times N\}$. Traditionally [2, 15, 16], these orthogonal grid functions are normalized to one pixel width and lexicographically ordered by multiindex $k = (q,n) = 1, 2,\dots,K = Q\times N$. Hence, the K-d approximation of the scattering field becomes

$$e_{(K)}(\mathbf{x}) = (P_{E(K)}e)(\mathbf{x}) = \sum_{k=1}^{K} E_k g_k(\mathbf{x}), \tag{7}$$

where $P_{E(K)}$ represents a projector onto the K-d signal approximation subspace

$$E_{(K)} = P_{E(K)}E = \text{Span}\,\{g_k(\mathbf{x})\} \tag{8}$$

spanned by K-orthogonal grid functions (pixels) $\{g_k(\mathbf{x})\}$.

Using such approximations, we proceed from the operator-form EO (4) to its conventional vectorized form

$$\mathbf{U} = \mathbf{SE} + \mathbf{N}, \tag{9}$$

where $\mathbf{U}$, $\mathbf{N}$, and $\mathbf{E}$ define the vectors composed of the coefficients U_m, N_m, and E_k of the finite-dimensional approximations of the fields u, n, and e, respectively, and $\mathbf{S}$ is the matrix-form representation of the SFO with elements [4] $\{S_{mk} = [Sg_k, h_m]_U = \int_Y (Sg_k(\mathbf{x}))(\mathbf{y})h_m^*(\mathbf{y})d\mathbf{y};\ k = 1,\dots,K;\ m = 1,\dots,M\}$.

Zero-mean Gaussian vectors $\mathbf{E}$, $\mathbf{N}$, and $\mathbf{U}$ in (9) are characterized by the correlation matrices, $\mathbf{R_E}$, $\mathbf{R_N}$, and $\mathbf{R_U} = \mathbf{SR_ES}^+ + \mathbf{R_N}$, respectively, where superscript + defines the Hermitian conjugate when it stands with a matrix. Because of the incoherent nature of the scattering field $e(\mathbf{x})$, the vector $\mathbf{E}$ has a diagonal correlation matrix, $\mathbf{R_E} = \text{diag}\{\mathbf{B}\} = \mathbf{D}(\mathbf{B})$, in which the $K \times 1$ vector of the principal diagonal $\mathbf{B}$ is composed of elements $B_k = \langle E_k E_k^* \rangle$; $k = 1,\dots,K$. This vector $\mathbf{B}$ is referred to as a vector-form representation of the SSP, that is, the SSP vector [4, 14]. The K-d approximation of the SSP estimate $\hat{B}_{(K)}(\mathbf{x})$ as a continuous function of $\mathbf{x} \in X$ over the probing scene X is now expressed as follows:

$$\hat{B}_{(K)}(\mathbf{x}) = \text{est}\,\{\langle |e_{(K)}(\mathbf{x})|^2 \rangle\} = \sum_{k=1}^{K} \hat{B}_k g_k(\mathbf{x}); \quad \mathbf{x} \in X, \tag{10}$$

where $\text{est}\{f\} = \hat{f}$ defines the estimate of a function.

Analyzing (10), one may deduce that in every particular measurement scenario (specified by the corresponding approximation spaces $U_{(M)}$ and $E_{(K)}$) one has to derive the estimate $\hat{\mathbf{B}}$ of a vector-form approximation of the SSP that uniquely defines via (10) the approximated continuous SSP distribution $\hat{B}_{(K)}(\mathbf{x})$ over the observed scene $X \ni \mathbf{x}$.

3. SDR STRATEGY FOR SSP ESTIMATION

In the descriptive statistical formalism, the desired estimate of the SSP vector $\hat{\mathbf{B}}$ is recognized to be a vector that composes a principal diagonal of the estimate of the correlation

matrix $\mathbf{R}_{\mathbf{E}}(\mathbf{B})$; that is, $\hat{\mathbf{B}} = \{\hat{\mathbf{R}}_{\mathbf{E}}\}_{\text{diag}}$. Thus one can seek to estimate $\hat{\mathbf{B}} = \{\hat{\mathbf{R}}_{\mathbf{E}}\}_{\text{diag}}$ given the data correlation matrix $\mathbf{R}_{\mathbf{U}}$ preestimated by some means, for example, via averaging the correlations over J independent snapshots [1, 16]

$$\hat{\mathbf{R}}_{\mathbf{U}} = \mathbf{Y} = \underset{j\in J}{\text{aver}}\left\{\mathbf{U}_{(j)}\mathbf{U}_{(j)}^{+}\right\} = \frac{1}{J}\sum_{j=1}^{J}\mathbf{U}_{(j)}\mathbf{U}_{(j)}^{+} \tag{11}$$

by determining the solution operator that we also refer to as the image formation operator (IFO) $\mathbf{F}$ such that

$$\hat{\mathbf{B}} = \{\hat{\mathbf{R}}_{\mathbf{E}}\}_{\text{diag}} = \{\mathbf{F}\mathbf{Y}\mathbf{F}^{+}\}_{\text{diag}}. \tag{12}$$

To optimize the search of such IFO $\mathbf{F}$, we address the following SDR strategy: to design the IFO

$$\mathbf{F} \longrightarrow \min_{\mathbf{F}}\{\text{Risk}(\mathbf{F})\}, \tag{13}$$

that minimizes the composite objective function

$$\text{Risk}(\mathbf{F}) = \text{trace}\{(\mathbf{F}\mathbf{S}-\mathbf{I})\mathbf{A}(\mathbf{F}\mathbf{S}-\mathbf{I})^{+}\} + \alpha\,\text{trace}\{\mathbf{F}\mathbf{R}_{\mathbf{N}}\mathbf{F}^{+}\}, \tag{14}$$

where $\mathbf{I}$ defines an identity matrix.

We refer to the objective function defined by (14) as the composite descriptive risk. Such Risk($\mathbf{F}$) is composed of the weighted sum of the systematic error function specified as trace$\{(\mathbf{F}\mathbf{S}-\mathbf{I})\mathbf{A}(\mathbf{F}\mathbf{S}-\mathbf{I})^{+}\}$ (the first addend in Risk($\mathbf{F}$)) and the fluctuation error function specified as trace$\{\mathbf{F}\mathbf{R}_{\mathbf{N}}\mathbf{F}^{+}\}$ (the second addend in Risk($\mathbf{F}$)). These two functions define the systematic and fluctuation error measures in the desired solution $\hat{\mathbf{B}}$, correspondingly, and the regularization parameter α controls the balance between such two measures. The selection (adjustment) of the parameter α and the metrics or weight matrix $\mathbf{A}$ provides additional regularization degrees of freedom incorporating any descriptive properties of a solution if those are known a priori [8, 10], hence the accepted definition, *descriptive risk*. Thus, the proposed SDR strategy (13) implies minimization of the balanced composition of two error measures (systematic and fluctuation), that is, enhancement of the spatial resolution attained in the reconstructed image balanced with the admissible image degradation due to the impact of the resulting noise.

In the hypothetical case of a solution-dependent $\mathbf{A}$, for example, when $\mathbf{A} = \mathbf{D} = \text{diag}(\mathbf{B})$, the SDR strategy stated by (13) is recognized to coincide with the Bayes minimum risk (BMR) inference paradigm that optimally balances the spatial resolution and the noise energy in the resulting SSP estimate in the metrics adjusted to the a priori statistical information induced by the corresponding correlation matrices, $\mathbf{A} = \mathbf{D}$ and $\mathbf{R}_{\mathbf{N}}$, respectively [3]. In our case of estimating the SSP, the signal correlation matrix $\mathbf{R}_{\mathbf{E}} = \mathbf{D} = \mathbf{D}(\mathbf{B}) = \text{diag}\{\mathbf{B}\}$ is itself unknown (as that defines the SSP $\mathbf{B}$ to be estimated). That is why, in the SDR strategy, we propose to use any admissible (i.e., selfadjoint real-valued invertible) weight matrix $\mathbf{A}$; hence, we robustify the absence of the a priori knowledge about the SSP $\mathbf{B}$ via introducing the additional regularization degrees of freedom (selection of the matrix $\mathbf{A}$ and tolerance factor α) into the desired solution. Nevertheless, it is worthwhile to note that the proposed SDR strategy (13) admits also the use of the solution-dependent metrics (i.e., $\mathbf{A} = \hat{\mathbf{D}} = \text{diag}\{\hat{\mathbf{B}}\}$) that requires the adaptive structure of the resulting SSP estimator. All such structures are to be detailed later in Section 5.

4. UNIFIED SDR ESTIMATOR FOR SSP

Routinely solving the optimization problem (13), we obtain (see the appendix where this solution is detailed)

$$\mathbf{F} = \mathbf{K}_{\mathbf{A},\alpha}\mathbf{S}^{+}\mathbf{R}_{\mathbf{N}}^{-1}, \tag{15}$$

where

$$\mathbf{K}_{\mathbf{A},\alpha} = \left(\mathbf{S}^{+}\mathbf{R}_{\mathbf{N}}^{-1}\mathbf{S} + \alpha\mathbf{A}^{-1}\right)^{-1}. \tag{16}$$

For the solution operator (15) (i.e., for the image formation operator (IFO) defined by (15)), the minimal possible value of the descriptive risk function $\text{Risk}_{\min}(\mathbf{F}) = \text{tr}\{\mathbf{K}_{\mathbf{A},\alpha}\}$ is attained.

In the general case of arbitrary fixed α and $\mathbf{A}$, the unified SDR estimator of the SSP becomes

$$\begin{aligned}\hat{\mathbf{B}}_{FBR} &= \{\mathbf{K}_{\mathbf{A},\alpha}\mathbf{S}^{+}\mathbf{R}_{\mathbf{N}}^{-1}\mathbf{Y}\mathbf{R}_{\mathbf{N}}^{-1}\mathbf{S}\mathbf{K}_{\mathbf{A},\alpha}\}_{\text{diag}} \\ &= \left\{\mathbf{K}_{\mathbf{A},\alpha}\underset{j\in J}{\text{aver}}\{\mathbf{Q}_{(j)}\mathbf{Q}_{(j)}^{+}\}\mathbf{K}_{\mathbf{A},\alpha}\right\}_{\text{diag}},\end{aligned} \tag{17}$$

where $\mathbf{Q}_{(j)} = \{\mathbf{S}^{+}\mathbf{R}_{N}^{-1}\mathbf{U}_{(j)}\}$ is recognized to be an output of a matched spatial filter with preliminary noise whitening after processing the jth data snapshot; $j = 1,\ldots,J$ [1]. Although in practical scenarios the noise correlation matrix $\mathbf{R}_{\mathbf{N}}$ is usually unknown, it is a common practice in such cases to accept the robust white noise model, that is, $\mathbf{R}_{\mathbf{N}}^{-1} = (1/N_0)\mathbf{I}$, with the noise intensity N_0 preestimated by some means [1, 2].

5. FAMILY OF THE SDR-RELATED ESTIMATORS

5.1. Robust spatial filtering

Consider white zero-mean noise in observations and no preference to any prior model information; that is, putting $\mathbf{A} = \mathbf{I}$. Let the regularization parameter be adjusted as an inverse of the signal-to-noise ratio (SNR), for example, $\alpha = N_0/B_0$, where B_0 represents the prior average gray level of the SSP specified, for example, via image calibration [6]. In this case, the IFO $\mathbf{F}$ is recognized to be the Tikhonov-type robust spatial filtering (RSF) operator:

$$\mathbf{F}_{\text{RSF}} = \mathbf{F}^{(1)} = \left(\mathbf{S}^{+}\mathbf{S} + \frac{N_0}{B_0}\mathbf{I}\right)^{-1}\mathbf{S}^{+}. \tag{18}$$

5.2. Matched spatial filtering

Consider the model from the previous example for an assumption, $\alpha \gg \|\mathbf{S}^{+}\mathbf{S}\|$, that is, the case of a priority of suppression of the noise over minimization of the systematic error in the optimization problem (13). In this case, we can roughly approximate (18) as the matched spatial filtering (MSF) operator:

$$\mathbf{F}_{\text{MSF}} = \mathbf{F}^{(2)} \approx \text{const}\cdot\mathbf{S}^{+}. \tag{19}$$

5.3. Adaptive spatial filtering

Consider the case of zero-mean noise with an arbitrary correlation matrix $\mathbf{R_N}$, equal importance of two error measures in (14), that is, $\alpha = 1$, and the solution-dependent weight matrix $\mathbf{A} = \hat{\mathbf{D}} = \mathrm{diag}\{\hat{\mathbf{B}}\}$. In this case, the IFO $\mathbf{F}$ becomes the adaptive spatial filtering (ASF) operator:

$$\mathbf{F}_{\mathrm{ASF}} = \mathbf{F}^{(3)} = \left(\mathbf{S}^{+}\mathbf{R}_{\mathbf{N}}^{-1}\mathbf{S} + \hat{\mathbf{D}}^{-1}\right)^{-1}\mathbf{S}^{+}\mathbf{R}_{\mathbf{N}}^{-1} \tag{20}$$

that defines the corresponding solution-dependent ASF estimator

$$\hat{\mathbf{B}}_{\mathrm{ASF}} = \left\{\mathbf{F}^{(3)}\mathbf{Y}\mathbf{F}^{(3)+}\right\}_{\mathrm{diag}}. \tag{21}$$

In this paper, we refer to (21) with the corresponding IFO (20) as the first representation form for the ASF method.

5.4. MVDR version of the ASF algorithm

As it was shown in [4, Appendix B], the solution (IFO) operator $\mathbf{F}^{(3)}$ defined by (20) can be represented also in another equivalent form:

$$\mathbf{F}_{\mathrm{ASF}} = \mathbf{F}^{(4)} = \hat{\mathbf{D}}\mathbf{S}^{+}\mathbf{Y}^{-1}, \tag{22}$$

in which case, (17) with such a solution-dependent IFO (22) can be expressed as

$$\hat{\mathbf{B}}_{\mathrm{ASF}} = \left\{\hat{\mathbf{D}}\right\}_{\mathrm{diag}} = \left\{\mathbf{F}^{(4)}\mathbf{Y}\mathbf{F}^{(4)+}\right\}_{\mathrm{diag}} = \left\{\hat{\mathbf{D}}\mathbf{S}^{+}\mathbf{Y}^{-1}\mathbf{S}\hat{\mathbf{D}}\right\}_{\mathrm{diag}}. \tag{23}$$

From (23), it follows now that for a diagonal-form matrix $\hat{\mathbf{D}} = \mathrm{diag}\{\hat{\mathbf{B}}\}$, the desired $\hat{\mathbf{B}}_{\mathrm{ASF}}$ is to be found as a solution to the equation

$$\hat{\mathbf{D}} = \hat{\mathbf{D}}\,\mathrm{diag}\left\{\left\{\mathbf{S}^{+}\mathbf{Y}^{-1}\mathbf{S}\right\}_{\mathrm{diag}}\right\}\hat{\mathbf{D}}. \tag{24}$$

Solving this equation with respect to $\hat{\mathbf{B}}_{\mathrm{ASF}} = \{\hat{\mathbf{D}}\}_{\mathrm{diag}}$, we obtain the second representation form for the same ASF estimator

$$\hat{\mathbf{B}}_{\mathrm{ASF}} = \left\{\mathbf{F}^{(4)}\mathbf{Y}\mathbf{F}^{(4)+}\right\}_{\mathrm{diag}} = \left\{\left[\mathrm{diag}\left\{\left\{\mathbf{S}^{+}\mathbf{Y}^{-1}\mathbf{S}\right\}_{\mathrm{diag}}\right\}\right]^{-1}\right\}_{\mathrm{diag}} \tag{25}$$

that coincides with the celebrated minimum variance distortionless response (MVDR) method [1],

$$\hat{B}_{k\,\mathrm{MVDR}} = \left(\mathbf{s}_k^{+}\mathbf{Y}^{-1}\mathbf{s}_k\right)^{-1}; \quad k = 1,\ldots,K. \tag{26}$$

In (26), $\mathbf{s}_k$ represents the so-called *steering vector* [1] for the kth look direction, which in our notational conventions is essentially the kth column vector of the SFO matrix $\mathbf{S}$.

Examining the formulae (20) and (22), one may easily deduce that $\mathbf{F}^{(3)} = \mathbf{F}^{(4)}$. Thus, on one hand, the celebrated MVDR estimator (26) may be viewed as a convenient practical form of implementing the ASF algorithm derived here in a framework of the SDR strategy. On the other hand, it is obvious now that the MVDR beamformer may be considered as a particular case of the derived above unified SDR image formation algorithm (17) under the solution-dependent metrics model assumptions $\mathbf{A} = \mathrm{diag}\{\hat{\mathbf{B}}\}$ with the uniform tolerance factor $\alpha = 1$, that result in the ASF method.

6. COMPUTER SIMULATIONS AND DISCUSSIONS

We simulated a conventional side-looking SAR with the fractionally synthesized aperture; that is, the array was synthesized by the moving antenna. The SFO of such a SAR is factored along two axes in the image plane [14]: the azimuth (horizontal axis, x_1) and the range (vertical axis, x_2). In the simulations, we considered the conventional triangular SAR range ambiguity function (AF) $\Psi_r(x_2)$ and Gaussian approximation; that is, $\Psi_a(x_1) = \exp(-(x_1)^2/a^2)$, of the SAR azimuth AF with the adjustable fractional parameter a [15]. Note that in the imaging radar theory [2, 14] the AF is referred to as the continuous-form approximation of the ambiguity operator matrix $\mathbf{\Psi} = \mathbf{S}^{+}\mathbf{S}$ and serves as an equivalent to the point spread function in the conventional image processing terminology [6, 8]. In this paper, we present the simulations performed with two characteristic scenes. The first one, of the 256-by-180 pixel format, was borrowed from the artificial SAR imagery of the urban areas [15]. The second one, of the 512-by-512 pixel format, was borrowed from the real-world terrain SAR imagery (south-west Guadalajara region, Mexico [17]). The first scene was used as a test for adjustment of the RSF and ASF algorithms to attain the desired improvement in the image enhancement performances (the IOSNR defined below). In the reported simulations, the resolution cell along the x_2 direction was adjusted to the effective width of the range AF for both simulated scenarios. In the x_1 direction, the fractional parameter a was controlled to adjust different effective widths $\Delta\Psi_a(x_1)$ of the azimuth AF. Figure 1(a) shows the numerically modeled high-resolution hypothetical (not observed) image of the first original scene of the 256-by-180 pixel format. The simulations of SAR imaging of this scene and computer-aided image enhancement that employ the IFOs given by (19), (18), and (20) are displayed in Figures 1(b), 1(c), and 1(d), respectively. The enhanced images presented in Figures 1(c) and 1(d) were numerically reconstructed from the rough image of Figure 1(b) for the case of white Gaussian observation noise with the signal-to-noise ratio (SNR) $\mu = 20$ dB and the fractional parameter a adjusted to provide the horizontal width $\Delta\Psi_a(x_1)$ of the discretized azimuth AF $\Psi_a(x_1)$ at half of its peak level equal to 4 pixels.

For the purpose of objectively testing the performances of different SDR-related SSP estimation algorithms, a quantitative evaluation of the improvement in the SSP estimates (gained due to applying the suboptimal and optimal IFOs $\mathbf{F}^{(1)}$ and $\mathbf{F}^{(3)}$ instead of the adjoint operator $\mathbf{F}^{(2)} = \mathbf{S}^{+}$) was accomplished. In analogy to image reconstruction [15, 16], we use the quality metric defined as an improvement in the output signal-to-noise ratio (IOSNR),

$$\begin{aligned}
\mathrm{IOSNR}^{(\mathrm{RSF})} &= 10\log_{10}\frac{\sum_{k=1}^{K}\left(\hat{B}_k^{(\mathrm{MSF})} - B_k\right)^2}{\sum_{k=1}^{K}\left(\hat{B}_k^{(\mathrm{RSF})} - B_k\right)^2};\\
\mathrm{IOSNR}^{(\mathrm{ASF})} &= 10\log_{10}\frac{\sum_{k=1}^{K}\left(\hat{B}_k^{(\mathrm{MSF})} - B_k\right)^2}{\sum_{k=1}^{K}\left(\hat{B}_k^{(\mathrm{ASF})} - B_k\right)^2},
\end{aligned} \tag{27}$$

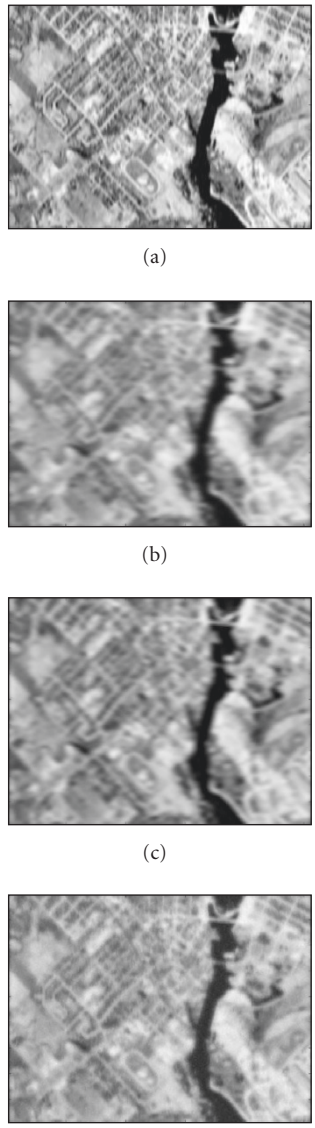

(a)

(b)

(c)

(d)

Figure 1: Simulation results with the first test scene: (a) original high-resolution numerically modeled scene image (not observed in the imaging experiment); (b) scene image formed applying the MSF method (simulated observed low-resolution noised image); (c) scene image enhanced with the RSF method; (d) scene image optimally enhanced applying the ASF method.

where B_k represents a value of the kth element (pixel) of the original SSP $\mathbf{B}$, $\hat{B}_k^{(\mathrm{MSF})}$ represents a pixel value of the kth element (pixel) of the rough SSP estimate $\hat{\mathbf{B}}_{\mathrm{MSF}}$, $\hat{B}_k^{(\mathrm{RSF})}$ represents a value of the kth pixel of the suboptimal SSP estimate $\hat{\mathbf{B}}_{\mathrm{RSF}}$, and $\hat{B}_k^{(\mathrm{ASF})}$ corresponds to the kth pixel value of the SDR-optimised SSP estimate $\hat{\mathbf{B}}_{\mathrm{ASF}}$, respectively. IOSNR$^{(\mathrm{RSF})}$ corresponds to the RSF estimator and IOSNR$^{(\mathrm{ASF})}$ corresponds to the ASF method. According to (27), the higher the IOSNR is, the better the improvement in the SSP estimate is, that is, the closer the estimate is to the original SSP.

Table 1: IOSNR values provided with the two simulated methods: RSF and ASF. The results are reported for two SAR system models with different resolution parameters and different SNRs.

SNR	First system		Second system	
μ	$\Delta\Psi_a = 4$		$\Delta\Psi_a = 10$	
	IOSNR$^{(\mathrm{RSF})}$	IOSNR$^{(\mathrm{ASF})}$	IOSNR$^{(\mathrm{RSF})}$	IOSNR$^{(\mathrm{ASF})}$
[dB]	[dB]	[dB]	[dB]	[dB]
15	2.17	3.13	2.55	3.82
20	3.27	4.25	4.39	5.71
25	4.13	5.05	5.24	7.35
30	5.48	6.17	6.38	9.12

In Table 1, we report the IOSNRs (in the dB scale) gained with the derived above RSF and ASF estimators for typical SAR system models that operate under different SNRs levels μ for two typical operation scenarios with different widths of the fractionally synthesised apertures: $\Delta\Psi_a(x_1) = 4$ pixels (first system) and $\Delta\Psi_a(x_1) = 10$ pixels (second system). The higher values of IOSNR$^{(\mathrm{RSF})}$ as well as IOSNR$^{(\mathrm{ASF})}$ were obtained in the second scenario. Note that IOSNR (27) is basically a squire-type error metric. Thus, it does not qualify quantitatively the "delicate" visual features in the images, hence, small differences in the corresponding IOSNRs reported in Table 1. In addition, both enhanced estimators manifest the higher IOSNRs in the case of more smooth azimuth AFs (larger values of $\Delta\Psi_a(x_1)$) and higher SNRs μ.

Finally, the qualitative results of the simulations of the same MSF, RSF, and ASF imaging algorithms in their application to the second scene (borrowed from the real-world SAR imagery [17]) are displayed in Figures 2(a), 2(b), and 2(c), respectively, where the horizontal width $\Delta\Psi_a(x_1)$ of the discretized azimuth AF $\Psi_a(x_1)$ at half of its peak level was adjusted now to 10 pixels of the 512-by-512 image pixel format (second simulated operation scenario).

The advantage of the SDR-reconstructed images (cases $\hat{\mathbf{B}}_{\mathrm{RSF}}$ and $\hat{\mathbf{B}}_{\mathrm{ASF}}$) over the conventional case $\hat{\mathbf{B}}_{\mathrm{MSF}}$ is evident in both simulated scenarios. Due to the performed regularized SFO inversions, the resolution was improved in the both cases, $\hat{\mathbf{B}}_{\mathrm{RSF}}$ and $\hat{\mathbf{B}}_{\mathrm{ASF}}$, respectively. The SDR-optimized reconstructed (ASF), in addition, manifests the reduced ringing effects, while the robust SDR estimator (RSF) with the IFO given by (18) did not require adaptive iterative computing, thus resulted in the processing with substantial reduced computational load (e.g., in the reported simulations, the RSF algorithm required approximately 40 times less computations than the ASF (23) (or MVDR (26)). These results qualitatively demonstrate that with some proper adjustment of the degrees of freedom in the general SDR-optimized estimator (17), one could approach the quality of the MVDR image formation method avoiding the cumbersome adaptive computations. Such optimization is a matter of the further studies.

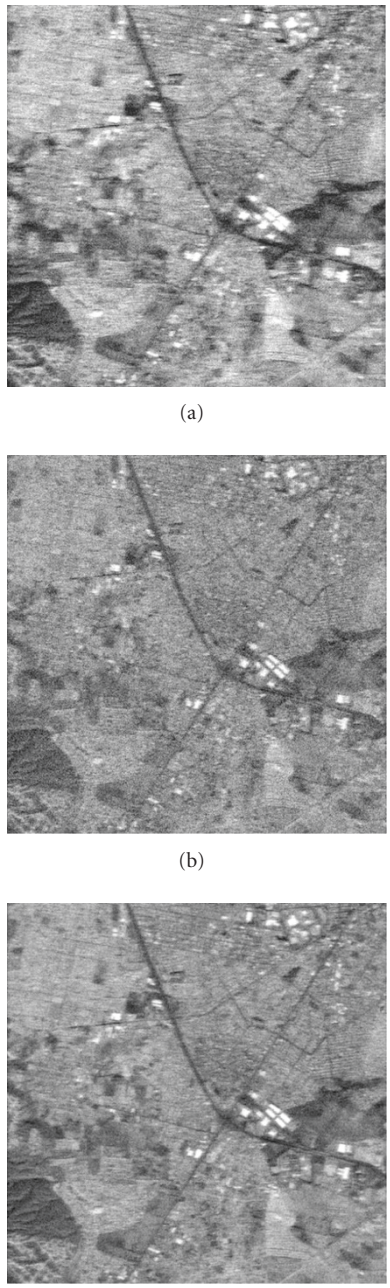

(a)

(b)

(c)

Figure 2: Simulation results with the second scene: (a) acquired SAR image (formed applying the MSF method); (b) scene image enhanced with the RSF method; (c) scene image optimally enhanced applying ASF method.

7. CONCLUDING REMARKS

In this paper, we have presented the fused statistical descriptive regularization (SDR) approach for solving the nonlinear inverse problem of estimation of the SSP of the backscattered wavefields via space-time processing of the finite-dimensional space-time measurements of the imaging radar signals as it is required, for example, for enhanced remote sensing imaging with array radar/SAR. Our study revealed some new aspects of designing the optimal/suboptimal SSP estimators and imaging techniques important for both the theory and practical implementation. To derive the optimal SSP estimator, we proposed the fused SDR strategy that incorporated the nontrivial a priori information on the desired SSP through unifying the regularization considerations with the minimum risk statistical estimation paradigm. Being nonlinear and solution dependent, the general optimal solution-dependent SDR estimator requires adaptive signal processing operations that result in a rather cumbersome computing. The computational complexity arises due to the necessity to perform simultaneously the solution-dependent operator inversions with control of the regularization degrees of freedom. However, we have proposed a robustified approach for some simplifications of the general SDR-optimal ASF estimator that leads to the computationally efficient RSF method. In the terms of regularization theory, this method may be interpreted as robustified image enhancement/reconstruction technique. Indeed, with an adequate selection of some design parameters that contain the RSF and ASF estimators, the remotely sensed image performances can be substantially improved if compared with those obtained using the conventional MSF method that is traditionally implemented in all existing remote sensing and imaging systems that employ the array sensor radars, side looking airborne radars, or SAR. This was demonstrated in the simulation experiment of enhancement of the SAR images related to some typical remote sensing operational scenarios.

APPENDIX

DERIVATION OF THE FUSED SDR-OPTIMAL IMAGE FORMATION (SOLUTION) OPERATOR (15)

The problem to be resolved in this appendix is to derive the solution operator (i.e., the IFO) that is optimal in a sense of the SDR strategy; that is,

$$\begin{aligned}\mathbf{F} &\longrightarrow \min_{\mathbf{F}} \{\,\mathrm{Risk}(\mathbf{F})\} \\ &\longrightarrow \min_{\mathbf{F}} \{\,\mathrm{trace}\,\{(\mathbf{FS}-\mathbf{I})\mathbf{A}(\mathbf{FS}-\mathbf{I})^{+}\} + \alpha\,\mathrm{trace}\,\{\mathbf{FR_N F}^{+}\}\}.\end{aligned} \tag{A.1}$$

To determine the optimum solution operator, $\mathbf{F}$, we have to differentiate the objective function, $\mathrm{Risk}(\mathbf{F})$, with respect to $\mathbf{F}$, set the result to zero, and solve the corresponding variational equation. To proceed with calculations, we, first, decompose the first addend in the risk function using the formula, $\mathbf{FSA}(\mathbf{FS})^{+} = \mathbf{FSAS}^{+}\mathbf{F}^{+}$, and rewrite (A.1) as follows:

$$\begin{aligned}\mathbf{F} \longrightarrow \min_{\mathbf{F}}\{\,&\mathrm{trace}\{\mathbf{FSAS}^{+}\mathbf{F}^{+}\} \\ &- [\,\mathrm{trace}\,\{\mathbf{FSA}\} + \mathrm{trace}\,\{\mathbf{AS}^{+}\mathbf{F}^{+}\}\,] \\ &+ \mathrm{trace}\{\mathbf{A}\} + \alpha\,\mathrm{trace}\,\{\mathbf{FR_N F}^{+}\}\}.\end{aligned} \tag{A.2}$$

Next, we invoke the following formulae for differentiating the traces of the composition of matrices with respect to a matrix:

$$\begin{aligned}\frac{\partial \operatorname{trace}\{\mathbf{FCF}^{+}\}}{\partial \mathbf{F}} &= 2\mathbf{FC},\\ \frac{\partial\{\operatorname{trace}\{\mathbf{FT}\}+\operatorname{trace}\{\mathbf{T}^{+}\mathbf{F}^{+}\}\}}{\partial \mathbf{F}} &= 2\mathbf{T}^{+}.\end{aligned} \tag{A.3}$$

To apply these formulae for solving the minimization problem (A.2), we associate $\mathbf{C}$ with $\mathbf{SAS}^{+}$ for the first addend from (A.2) and with $\mathbf{R_N}$ for the last addend from (A.2), correspondingly, while $\mathbf{T}$ is associated with $\mathbf{SA}$. Also, in calculations, we take into account that the $\mathbf{A}$ is a selfadjoint real-valued square matrix; that is, $\mathbf{A} = \mathbf{A}^{+}$, hence $\mathbf{T}^{+} = \mathbf{AS}^{+}$.

Following the specified above notational conventions, we apply now formulae (A.3) to (A.2) to get the expression for the matrix derivative $\partial\{\text{Risk}(\mathbf{F})\}/\partial\mathbf{F}$ and then set the result to zero. This yields the following variational equation:

$$\begin{aligned}\frac{\partial\{\text{Risk}(\mathbf{F})\}}{\partial \mathbf{F}} &= 2\mathbf{FSAS}^{+} - 2\mathbf{AS}^{+} + 2\alpha\mathbf{FR_N}\\ &= 2(\mathbf{FS}-\mathbf{I})\mathbf{AS}^{+} + 2\alpha\mathbf{FR_N} = \mathbf{0}.\end{aligned} \tag{A.4}$$

Rearranging (A.4), we obtain

$$\mathbf{F}\left(\mathbf{SAS}^{+} + \alpha\mathbf{R_N}\right) = \mathbf{AS}^{+} \tag{A.5}$$

that yields the desired solution (IFO) operator in its initial form,

$$\mathbf{F} = \mathbf{AS}^{+}\left(\mathbf{SAS}^{+} + \alpha\mathbf{R_N}\right)^{-1}. \tag{A.6}$$

Next, we make use of the dual form of representation of the matrix composition defined by (A.6):

$$\begin{aligned}\mathbf{F} &= \mathbf{AS}^{+}\left(\mathbf{SAS}^{+} + \alpha\mathbf{R_N}\right)^{-1}\\ &= \left(\mathbf{S}^{+}\mathbf{R_N^{-1}}\mathbf{S} + \alpha\mathbf{A}^{-1}\right)^{-1}\mathbf{S}^{+}\mathbf{R_N^{-1}},\end{aligned} \tag{A.7}$$

detailed, for example, in [4, Appendix B] that results in the desired solution operator

$$\mathbf{F} = \mathbf{K}_{\mathbf{A},\alpha}\mathbf{S}^{+}\mathbf{R_N^{-1}} \tag{A.8}$$

with

$$\mathbf{K}_{\mathbf{A},\alpha} = \left(\mathbf{S}^{+}\mathbf{R_N^{-1}}\mathbf{S} + \alpha\mathbf{A}^{-1}\right)^{-1}; \tag{A.9}$$

that is, the desired solution operator (IFO) defined by (15), (16). Such solution (IFO) operator (A.8) is recognized to be a composition of the whitening filter (defined by operator $\mathbf{R_N^{-1}}$), matched filter (given by operator $\mathbf{S}^{+}$), and the $\mathbf{A}$-dependent and α-dependent reconstructive filter (specified by operator (A.9), i.e., $\mathbf{K}_{\mathbf{A},\alpha} = (\mathbf{S}^{+}\mathbf{R_N^{-1}}\mathbf{S} + \alpha\mathbf{A}^{-1})^{-1}$).

REFERENCES

[1] S. Haykin and A. Steinhardt, Eds., *Adaptive Radar Detection and Estimation*, John Wiley & Sons, NY, USA, 1992.

[2] F. M. Henderson and A. J. Lewis, Eds., *Principles and Applications of Imaging Radar: Manual of Remote Sensing*, vol. 2, John Wiley & Sons, New York, NY, USA, 3d edition, 1998.

[3] Y. Shkvarko and J. L. Leyva-Montiel, "Theoretical aspects of array radar imaging via fusing the experiment design and regularization techniques," in *Proceedings of the 2nd IEEE Sensor Array and Multichannel Signal Processing Workshop (SAM '02)*, pp. 115–119, Rosslyn, Va, USA, August 2002, CD ROM.

[4] Y. Shkvarko, "Estimation of wavefield power distribution in the remotely sensed environment: Bayesian maximum entropy approach," *IEEE Transactions on Signal Processing*, vol. 50, no. 9, pp. 2333–2346, 2002.

[5] P. Stoica and R. Moses, *Introduction to Spectral Analysis*, Prentice-Hall, Upper Saddle River, NJ, USA, 1997.

[6] J. L. Starck, F. Murtagh, and A. Bijaoui, *Image Processing and Data Analysis. The Multiscale Approach*, Cambridge University Press, Cambridge, UK, 1998.

[7] B. R. Mahafza, *Radar Systems Analysis and Design Using MATLAB*, CRC Press, Boca Raton, Fla, USA, 2000.

[8] M. G. Kang and A. K. Katsaggelos, "General choice of the regularization functional in regularized image restoration," *IEEE Transactios on Image Processing*, vol. 4, no. 5, pp. 594–602, 1995.

[9] J. Astola and P. Kuosmanen, *Fundamentals of Nonlinear Digital Filtering*, CRC Press, Boca Raton, Fla, USA, 1997.

[10] V. Z. Mesarovic, N. P. Galatsanos, and A. K. Katsaggelos, "Regularized constrained total least squares image restoration," *IEEE Transactions on Image Processing*, vol. 4, no. 8, pp. 1096–1108, 1995.

[11] A. W. Doerry, F. M. Dickey, L. A. Romero, and J. M. DeLaurentis, "Difficulties in superresolving synthetic aperture radar images," in *Algorithms for Synthetic Aperture Radar Imagery IX*, vol. 4727 of *Proceedings of SPIE*, pp. 122–133, Orlando, Fla, USA, April 2002.

[12] D. C. Bell and R. M. Narayanan, "Theoretical aspects of radar imaging using stochastic waveforms," *IEEE Transactions on Signal Processing*, vol. 49, no. 2, pp. 394–400, 2001.

[13] Y. Shkvarko, Y. S. Shmaliy, R. Jaime-Rivas, and M. Torres-Cisneros, "System fusion in passive sensing using a modified hopfield network," *Journal of the Franklin Institute*, vol. 338, no. 4, pp. 405–427, 2001.

[14] Y. Shkvarko, "Unifying regularization and Bayesian estimation methods for enhanced imaging with remotely sensed data—part I: theory," *IEEE Transactions on Geoscience and Remote Sensing*, vol. 42, no. 5, pp. 923–931, 2004.

[15] Y. Shkvarko, "Unifying regularization and Bayesian estimation methods for enhanced imaging with remotely sensed data—part II: implementation and performance issues," *IEEE Transactions on Geoscience and Remote Sensing*, vol. 42, no. 5, pp. 932–940, 2004.

[16] R. C. Puetter, "Information, language, and pixon-based image reconstruction," in *Digital Image Recovery and Synthesis III*, vol. 2827 of *Proceedings of SPIE*, pp. 12–31, Denver, Colo, USA, August 1996.

[17] Y. Shkvarko and I. E. Villalon-Turrubiates, "Intelligent processing of remote sensing imagery for decision support in environmental resource management: a neural computing paradigm," in *Proceedings of Information Resource Management Association International Conference (IRMA '05)*, San Diego, Calif, USA, May 2005, CD ROM.

Yuriy Shkvarko (IEEE Member in 1995, IEEE Senior Member in 2004) received the Dipl. Eng. degree (with honors) in radio engineering in 1976, the Candidate of Sciences degree (Ph.D. degree equivalent in the ex-USSR) in radio systems in 1980, and the Doctor of Sciences degree (doctoral grade of excellence in the ex-USSR) in radio physics, radar, and navigation in 1990, all from the Supreme Evaluation Commission of the Council of Ministers of the ex-USSR (presently Russia). From 1976 to 1991, he was with the Scientific Research Department of the Kharkov Aviation Institute, Kharkov, ex-USSR, as a Research Fellow, Senior Fellow, and finally as a Chair of the Research Laboratory in information technologies for radar and navigation. From 1991 to 1999, he was a Professor at the Department of System Analysis and Control of the Ukrainian National Polytechnic Institute at Kharkov, Ukraine. From 1999 to 2001, he was a Visiting Professor in the Guanajuato State University at Salamanca, Mexico. In 2001, he joined the Guadalajara Unit of the CINVESTAV (Center for Advanced Research and Studies) of Mexico as a Titular Professor. His research interests are in applications of signal processing to remote sensing, imaging radar, and navigation and communications. He holds 12 patents from the ex-USSR, and has published two books and some 120 papers in journals and conference records on these topics. He is a Senior Member of the Mexican National System of Investigators and a Regular Member of the Mexican National Academy of Sciences.